Rac rather than Rho drives the early transcriptional response to extracellular matrix stiffness and mediates repression of ATF3

Irène Dang[1,2,*], Yongho Bae[1,3,*], Joseph A. Brazzo[3], and Richard K Assoian[1,2]

[1]Department of Systems Pharmacology and Translational Therapeutics and the [2]Center for Engineering MechanoBiology, University of Pennsylvania, Philadelphia PA 19104; [3]Department of Pathology and Anatomical Sciences, Jacobs School of Medicine and Biomedical Sciences, University at Buffalo, State University of New York, Buffalo, NY 14203

*co-first authors

YB present address: Department of Pathology and Anatomical Sciences, Jacobs School of Medicine and Biomedical Sciences, University at Buffalo, State University of New York, Buffalo, NY 14203

Address correspondence to: Richard K. Assoian

Tel: 215-898-7157
email: assoian@pennmedicine.upenn.edu

SUMMARY

The Rho family GTPases, Rac and Rho, play critical roles in transmitting mechanical information contained within the extracellular matrix (ECM) to the cell. Rac and Rho have well described roles in regulating stiffness-dependent actin remodeling, proliferation and motility. However, much less is known about the relative roles of these GTPases in stiffness-dependent transcription, particularly at the genome-wide level. Here, we selectively inhibited Rac and Rho in mouse embryonic fibroblasts cultured on deformable substrata and used RNA sequencing to elucidate and compare the contribution of these GTPases to the early transcriptional response to ECM stiffness. Surprisingly, we found that Rac activation is almost exclusively responsible for the initial transcriptional response to ECM stiffness. We also identified Activating Transcription Factor 3 (ATF3) as a major target of stiffness/Rac signaling and show that ATF3 repression by ECM stiffness connects the stiffness-dependent activation of Rac to the induction of cyclin D1.

INTRODUCTION

Cell adhesion to its surrounding extracellular matrix (ECM) is essential for viability, motility and proliferation of many cell types. The ECM is complex and composed of both protein and non-proteinaceous components. Adhesion to the ECM provides chemical information to the cell because many distinct ECM components bind to specific receptors on the cell surface to regulate intracellular signaling, often in concert with growth factor/cytokine-mediated activation of receptor tyrosine kinases (Boudreau and Jones, 1999; Assoian and Schwartz, 2001; Larsen *et al.*, 2006). Additionally, more recent work has shown that the ECM also provides mechanical information to the cell, and the rigidity or stiffness of the ECM affects many of the signaling events and cellular fates originally attributed to cell adhesion (Discher *et al.*, 2005; Suresh, 2007; Janmey *et al.*, 2015). Cells can sense the stiffness of their microenvironment when ECM proteins such as the fibrillar collagens bind to their specific cell surface receptors in the integrin family (Lee and Juliano, 2004; Bourgot *et al.*, 2020; Tang, 2020; Sun, 2021). Other ECM proteins such as fibronectin (FN) and vitronectin also bind to specific integrins and contribute to the information content of the cell's microenvironment.

The cytoplasmic domain of integrins lacks intrinsic kinase activity, but they associate directly and indirectly with a number of signaling molecules in dynamic macromolecular structures called focal complexes (FCs) and focal adhesions (FAs). FCs are near the cell periphery and unstable but mature into FAs under force (Geiger and Bershadsky, 2001; Geiger and Yamada, 2011; Burridge and Wittchen, 2013; Burridge and Guilluy, 2016; Wolfenson *et al.*, 2018). FAs contain many signaling molecules (Sastry and Burridge, 2000; Zaidel-Bar *et al.*, 2007; Horton *et al.*, 2016) and are also non-covalently linked to actin stress fibers, which mediate actomyosin contraction, generate intracellular tension, and reinforce FA maturation and stabilization (Geiger and Bershadsky, 2001; Geiger and Yamada, 2011; Lessey *et al.*, 2012; Burridge and Wittchen, 2013; Burridge and Guilluy, 2016; Wolfenson *et al.*, 2018). Thus, increased ECM stiffness promotes FA formation and regulates cytoplasmic signaling pathways that control mechanotransduction to the nucleus and a number of stiffness-sensitive cell fates including motility, differentiation, proliferation and transformation (Paszek *et al.*, 2005; Yeung *et al.*, 2005; Engler *et al.*, 2006; Assoian and Klein, 2008; Zajac and Discher, 2008; Janmey *et al.*, 2015; Wei *et al.*, 2015; Talwar *et al.*, 2021).

The Rac and Rho GTPases have pleiotropic effects on cells and tissues and are often involved in mechanosensitive signaling pathways and influence the cell fates described above (Zohn *et al.*, 1998; Sahai and Marshall, 2003; Burridge and Wennerberg, 2004; Hall, 2005; Provenzano and Keely, 2011; Lawson and Burridge, 2014; Pasapera *et al.*, 2014; Ridley, 2015). Rac activation is critical for FC formation and cell spreading while Rho activity has an established role in stress fiber and FA formation and enforcement (Zohn *et al.*, 1998; Sahai and Marshall, 2003; Burridge and Wennerberg, 2004; Hall, 2005; Provenzano and Keely, 2011; Lawson and Burridge, 2014; Pasapera *et al.*, 2014; Ridley, 2015). Both Rac and Rho play important roles in cell motility (Sahai and Marshall, 2003; Raftopoulou and Hall, 2004; Hall, 2005; Lawson and Burridge, 2014; Ridley, 2015). In contrast, we have previously reported that the activation of Rac, but not Rho, is required for stimulatory effects of ECM stiffness in G1 phase cell cycle progression (Klein *et al.*, 2009; Bae *et al.*, 2014). In this signaling pathway, the stiffness-dependent activation of FAK within FAs leads to the activation of p130Cas and eventually DOCK180, a Rac guanine

nucleotide exchange factor. The consequent stiffness-dependent activation of Rac and induction of lamellipodin is required for the mid-G1 phase expression of cyclin D1 (Klein *et al.*, 2009; Bae *et al.*, 2014; Brazzo *et al.*, 2021). Among its effects, cyclin D1 is perhaps best understood as an activator of cyclin-dependent kinase 4/6, which in turn, contributes to the release of E2Fs from the retinoblastoma protein family and promotes S phase entry (Sherr, 1993, 1995; Resnitzky and Reed, 1995; Weinberg, 1995). Thus, the stiffness-dependent activation of Rac plays an important role in the stimulatory effect of ECM stiffness on cell cycling. The third Rho family GTPase, Cdc42, is responsible for filopodia formation and directional motility (Cerione, 2004; Raftopoulou and Hall, 2004; Hall, 2005; Ridley, 2006), but its role in mechano-sensitive cell fates is not as well understood.

In addition to their effects on cytoplasmic signaling, both Rac and Rho have been reported to regulate transcription. The transcriptional effect is best understood for Rho, as stimulatory effects of Rho on actin polymerization lead to nuclear translocation of the MAL (also referred to as myocardin-related transcription factors and megakaryoblastic leukemia-1 and -2) co-activator of SRF genes (Sotiropoulos *et al.*, 1999; Miralles *et al.*, 2003; Pipes *et al.*, 2006; Parmacek, 2007; Zhao *et al.*, 2007). Additionally, both Rho and Rac have been implicated in the nuclear translocation of the YAP/Taz transcriptional coactivators (Dupont *et al.*, 2011; Aragona *et al.*, 2013; Jang *et al.*, 2017; Talwar *et al.*, 2021). Nevertheless, much remains unknown about the relative contributions of Rac and Rho to the transcriptional response to ECM stiffness, particularly at the genome-wide scale. To address this gap in understanding, we used next generation sequencing to determine and compare the effects of Rac versus Rho on the early transcriptional response to ECM stiffness. Despite the fact that Rac and Rho have similar effects on intracellular stiffness, we find that Rac is almost completely responsible for the initial transcriptional response to ECM stiffness. Additionally, we show that the levels of Activating Transcription Factor 3 (ATF3) are repressed by both high ECM stiffness and increased Rac activity. Stiffness-mediated ATF3 repression links mechanosensitive activation of Rac to cyclin D1 gene expression and S phase entry.

RESULTS

Rac and Rho similarly affect intracellular stiffness during early stages of cell adhesion and spreading

To compare the effects of Rac and Rho on the early transcriptional response to ECM stiffness, we treated serum-starved mouse embryo fibroblasts (MEFs) with drugs that acutely and specifically inhibit either Rac (EHT1864, a potent Rac family GTPase inhibitor) or Rho (CT04, cell permeable Rho inhibitor). We plated these drug-treated cells on fibronectin (FN)-coated polyacrylamide hydrogels in the presence of fetal bovine serum (FBS), using a hydrogel stiffness that mimics the stiffness found at sites of proliferation *in vivo* (20-25 kPa; hereafter called "stiff") (Klein *et al.*, 2009). This stiffness range also promotes motility and S-phase entry in cultured cells (Klein *et al.*, 2009; Bae *et al.*, 2014; Razinia *et al.*, 2017; Shutova *et al.*, 2017). We also used a lower stiffness (4-6 kPa; hereafter called "soft") that failed to stimulate proliferation and motility (Klein *et al.*, 2009; Bae *et al.*, 2014; Razinia *et al.*, 2017; Shutova *et al.*, 2017). MEFs were cultured for 1 h before collection and analysis. Using this approach, we tested EHT1864 and CT04 for their ability to inhibit the stiffness-dependent GTP-loading of Rac and Rho, respectively. We identified

concentrations of these drugs that resulted in strong inhibition of the respective GTPase target without significant effect on the other Rho family GTPases (Fig. 1A). F-actin abundance was reduced in response to both EHT1864 and CT04 (Fig. 1B-C). In addition, Rac, but not Rho, inhibition reduced cell area (Fig. 1B and 1D), a consequence of impaired cell spreading (Fig. S1). Importantly, both Rac and Rho inhibition similarly reduced intracellular stiffness as measured by atomic force microscopy (Fig. 1E).

Rac dominates the early transcriptional response to ECM stiffness and mediates the stiffness-dependent repression of ATF3

Using the experimental conditions identified in Fig. 1, we performed an RNA sequencing (RNASeq) to interrogate the relative roles of Rac and Rho in transducing the early transcriptional response to ECM stiffness. The results showed that of 483 genes stimulated by ECM stiffness, one third (158 genes) were inhibited by EHT1864, but only 1% (6 genes) were inhibited by CT04 (Fig. 2A and Table S1). Similarly, Rac was dominant over Rho when examining the genes that were inhibited by ECM stiffness (Fig. 2B and Table S2): about 40% of stiffness-inhibited genes showed an increased abundance in response to EHT1864 (123 of 327) but only 6% showed increased abundance in response to CT04 (19 of 327). Very few stiffness-regulated genes were affected by both the Rac and Rho inhibitors (Fig. 2A-B and Tables S1 and S2). Moreover, Fisher exact tests showed that the overlap between the stiffness-regulated and EHT1864-regulated genes was significant ($p<0.0001$ and 0.019 for the stiffness-stimulated and -inhibited, genes respectively) whereas the overlap between stiffness-regulated genes and the few CT04-regulated genes was not significant ($p=0.2$ and 0.31 for stiffness-stimulated and -inhibited, genes respectively). Thus, Rac rather than Rho drives the early transcriptional program in response to ECM stiffness.

Several studies have demonstrated a role for Rho signaling in mechanosensitive transcription, most commonly through MAL or YAP/Taz (see Introduction). The striking absence of Rho signals in our RNASeq data set does not question these findings but rather emphasizes that the *initial* transcriptional response to ECM stiffness is mediated by Rac, not Rho.

In an effort to better understand this genome-wide response, we searched for transcriptional regulators within the set of genes that were inversely regulated by ECM stiffness and Rac. The 158 genes that were stimulated by ECM stiffness and inhibited by EHT1864 (refer to Fig. 2A) and the 123 genes that were inhibited by ECM stiffness and stimulated by EHT1864 (refer to Fig. 2B) were compared to the Gene Ontology (GO) lists of transcription factors, transcriptional co-regulators, and histone modifiers (Figs. 2C-D and Table S3). The overlapping genes (34 and 10 in Fig. 2C and 2D, respectively) were then graphed by fold-change and adjusted p-value to visualize the relative robustness of their responses to ECM stiffness and Rac inhibition with EHT1864 (Fig. 2E-F and Table S4). The results showed that, as a group, neither transcription co-regulators nor histone modifiers were strongly regulated during the initial genome-wide response to ECM stiffness and Rac. However, the mRNAs for two transcription factors (Klf2 and ATF3) were repressed by ECM stiffness with high statistical significance (Fig. 2E). Of those two, the repression of ATF3 mRNA was much more robustly reversed by inhibition of Rac activity with EHT1864 (Fig. 2F). Note that Figs. 2E-F also revealed a strong effect of ECM stiffness and Rac inhibition on the expression level of Dnajb1 mRNA. Though associated with fibrolamellar carcinoma as a fusion protein (Dinh *et al.*, 2022), relatively little is known about Dnajb1 biology, and we therefore decided to focus our further studies on ATF3.

RT-qPCR confirmed that ATF3 mRNA levels were downregulated by culturing MEFs on a stiff substratum and strongly upregulated by treatment with EHT1864; the response to CT04 was not significantly different from the controls (Fig. 2G). Immunoblotting showed a similar repression of ATF3 protein abundance in response to ECM stiffness, and this effect was partially reversed when Rac-inhibited cells were cultured on a stiff ECM (Fig. 2G-I).

Stiffness/Rac-mediated repression of ATF3 linked to the expression of cyclin D1

ATF3 belongs to the ATF/CREB family of transcription factors, has pleiotropic effects on cells, and is canonically induced in response to various stress signals (Hai *et al.*, 1989; Hai and Hartman, 2001; Fan *et al.*, 2002; Rohini *et al.*, 2018; Ku and Cheng, 2020). Intriguingly, ATF3 has also been described as a repressor of cyclin D1 transcription, with direct binding to an inhibitory ATF3 site in the cyclin D1 promoter (James *et al.*, 2006; Lu *et al.*, 2006). As indicated above, cyclin D1 is a key regulator of progression through G1 phase, and we have previously shown that it is a major target of ECM stiffness-mediated signaling to the cell cycle (Klein *et al.*, 2009; Bae *et al.*, 2014). By plating FBS-stimulated MEFs on FN-coated hydrogels of increasing stiffness, we found that the levels of ATF3 mRNA (Fig. 3B) and cyclin D1 mRNA (Fig. 3C) both correlated with the level of Rac activity (Fig. 3A). In agreement with the results in Fig. 2, the correlation to Rac activity was inverse for ATF3 mRNA but direct for cyclin D1 mRNA.

We then compared the effect of Rac inhibition and activation on the expression of ATF3 and cyclin D1 mRNAs within the same lysates. RT-qPCR revealed a strong inverse correlation between the expression of ATF3 and cyclin D1 mRNAs in response to ECM stiffening (Fig. 4A; compare soft versus stiff). Moreover, both the stiffness-dependent repression of ATF3 mRNA and induction of cyclin D1 mRNA were reversed by Rac inhibition with EHT1864 (Fig. 4A; compare stiff ± EHT). Conversely, this inverse correlation was retained when we enforced Rac activity in MEFs on a soft ECM by ectopic expression of Rac^{V12}: the level of ATF3 mRNA decreased while that of cyclin D1 mRNA increased (Fig. 4B). Importantly, this inverse relationship between stiffness-dependent ATF3 repression and cyclin D1 induction is causal because forced expression of ATF3 in cells on stiff hydrogels was sufficient to block the stiffness-dependent induction of cyclin D1 (Fig. 4C-D).

Crispr-Cas9 methodology was used to delete ATF3 from MEFs and determine the effect on cyclin D1 and S-phase entry. We generated several ATF3-deficient clones (hereafter called ATF3 KO cells) as well as several control clones in which MEFs were transfected with a ROSA26 rather than ATF3 gRNA (Table S5 and Fig. S2A-B; red arrowheads). Phenotypically, the lack of ATF3 had no apparent effect on the cells, nor did we detect large changes in cell area or f-actin intensity (Fig. S2B-D). However, serum-stimulated ATF3 KO MEFs on stiff hydrogels displayed an increase in cyclin D1 expression (Fig. 4E-F), and this increase was associated with an increase in S phase entry as judged by the percentage of EdU positive nuclei (Fig. 4G; compare columns 1 and 3). Rac inhibition with EHT1864 reduced S phase entry in both the control the ATF-depleted MEFs (Fig. 4F; compare bars 1 to 2 and 3 to 4), indicating (not surprisingly) that Rac activity drives cyclin D1 expression by pathways beyond ATF3. Note, however, that the extent of S phase inhibition by EHT1864 was 30-fold in the ROSA controls (from 68% to 2%) but only 5-fold in the ATF3 KO MEFs (from 87% to 18%). Altogether, these data demonstrate that a stiffness- and Rac-dependent repression of ATF3 drives the induction of cyclin D1 (Fig. 4H). This effect

contributes not only to mechanosensitive cyclin D1 expression but also to the extent of S phase entry.

DISCUSSION

The stiffness (or rigidity) of the ECM is transduced into intracellular stiffness and mechanosensitive signaling. Rac and Rho are important regulators of mechanical signaling, but the relative transcriptional response to Rac and Rho at the genome-wide level is not well understood. We have examined this question by characterizing the effects of these GTPases on the ECM stiffness-mediated transcriptome.

Given the established role of Rho on nuclear translocation of the MAL and YAP transcriptional co-activators, we were surprised to find that Rho inhibition had almost no effect on the early transcriptional response to ECM stiffness. Rather, we found that Rac played a major role, and controlled about 30-40% of all genes regulated by a stiff ECM, both positively and negatively. However, it is important to emphasize that the relative contributions of Rac and Rho to mechanosensitive transcription are likely to be time-dependent, and the transcriptional contribution of Rho may increase as cells attach, spread, and develop force in response to stiff substrata.

Our unbiased analysis identified ATF3 as a major target of the early transcriptional responses to both ECM stiffness and Rac activity. We found that ATF3 mRNA levels are repressed by a stiff ECM stiffness and active Rac, and that this repression is important for the stiffness- and Rac-dependent induction of cyclin D1. ATF3 binds to the cyclic AMP response element (CRE) (consensus: 5'-GTGACGT[AC][AG]-3'), in numerous promoters and can act as a transcriptional activator or repressor (Hai *et al.*, 1989; Hai and Hartman, 2001; Fan *et al.*, 2002; Rohini *et al.*, 2018; Ku and Cheng, 2020). ATF3 homodimers can inhibit gene targets directly through an association with histone deacetylase 1, whereas ATF3-containing heterodimers can either positively or negatively regulate gene expression. ATF3 has also been described as both a positive and negative cell cycle regulator. While some reports suggest that ATF3 promotes cell proliferation (Allan *et al.*, 2001; Perez *et al.*, 2001), our results are in accordance with several other studies that have identified a negative role for ATF3 on cell cycle progression. For example, in addition to the inhibition of cyclin D1 gene expression as mentioned above, others have reported a repressive effect of ATF3 on cyclin A, cyclin E and Cdk2 levels, and ectopic expression of ATF3 suppresses cell cycle progression from G1 to S phase (Fan *et al.*, 2002; James *et al.*, 2006; Lu *et al.*, 2006). Use of different cell types and experimental conditions likely affect the cellular response to alterations in ATF3 levels. However, our use of substrata of physiologically relevant stiffness is likely providing additional insight that is not attainable when cells are cultured on rigid (glass or plastic) surfaces. Studies in 3D may provide even more insight. How the positive and negative cell cycle effects of ATF3 relate to ECM rigidity, dimensionality, time, and dimerization are important, but likely complex, matters to understand. Coordination between the stiffness effects on ATF3 expression as shown here and nuclear mechanosensing (Dahl *et al.*, 2008; Wang *et al.*, 2009; Swift and Discher, 2014; Kirby and Lammerding, 2018) will also be of interest.

Increased tissue stiffness, typically a result of ECM remodeling, is seen in many pathological microenvironments, such as breast and pancreatic tumors, lung and liver fibrosis, and

cardiovascular disease (Paszek *et al.*, 2005; Duprez and Cohn, 2007; Levental *et al.*, 2009; Liu *et al.*, 2010; Keely, 2011; Kothapalli *et al.*, 2012; Gehler *et al.*, 2013; Tung *et al.*, 2015; Piersma *et al.*, 2020; Zhang *et al.*, 2021; Maneshi *et al.*, 2021) and has even been considered as a prognostic factor in cancer progression (Wei and Yang, 2016; Reid *et al.*, 2017). Our data indicate that ATF3 is an early and major transcriptional target of increased ECM stiffness. Since ATF3 has widespread effects on cells, its downregulation by pathologically stiff microenvironments may be an early event that amplifies transcriptional misregulation in mechanosensitive pathologies.

METHODS

Cell culture, pharmacologic inhibition, ectopic expression, and GTPase activity assays

Spontaneous immortalized MEFs were cultured in DMEM-10% FBS at 37°C with 10% CO_2. For serum-starvation, near confluent monolayers were incubated for 48 h with DMEM-1 mg/ml heat-inactivated fatty-acid free BSA. The cells were cultured on polyacrylamide hydrogels, prepared as previously described (Klein *et al.*, 2007; Cretu *et al.*, 2010) on 12-mm, 25-mm or 40-mm coverslips and coated with FN (#341631, EMD) at 5 μg/ml. Hydrogel stiffness ranged from 2–4 kPa (low) to 20–24 (high) kPa. The coverslips were collected, and the cells were fixed for immunofluorescence (12-mm coverslips), or extracted for RNA (25-mm coverslips) or protein (40-mm coverslips).

Acute inhibition of Rac or Rho: MEFs were cultured in DMEM-10% FBS to 70-80% confluency and then serum-starved in DMEM-1 mg/ml BSA. After 48 h, the cells were trypsinized, resuspended in DMEM-1%BSA and incubated in suspension for 30 min at 37° C in 10% CO_2 and 2 μg/ml CT04 (#CT04-A, Cytoskeleton or 10 μM EHT1864 (#3872, Tocris). The vehicle control included the corresponding dilution of DMSO as needed. These pretreated cells were collected by gentle centrifuged, resuspended in DMEM-10% FBS, and plated on FN-coated hydrogels in the continued presence of inhibitor for 1 h.

Ectopic expression: MEFs were cultured at 70-80% confluency and infected with adenoviruses encoding Rac^{V12} (kind gift of Chris Chen, Boston University), Ad-GFP-h-ATF3 (Vector Biolabs), or GFP largely as described (Klein *et al.*, 2007; Bae *et al.*, 2014). The adenovirus dilutions used resulted in ~80% cell infection as judged by the GFP signal. The infected cells were washed with DMEM-1 mg/ml BSA, serum-starved, trypsinized, and plated on FN-coated polyacrylamide hydrogels as described above for 9 h for analysis by RT-qPCR and western blotting.

Rho family GTPases activity assay: Cells were treated with EHT1864 and CT04 as described above were collected, and Rac or Rho activity was assessed in duplicate using the G-LISA small G-protein activation assay kit (BK128, BK124, Cytoskeleton) according to the manufacturer's directions. Briefly, serum-starved MEFs were replated on fibronectin-coated low- and high-stiffness hydrogels and stimulated with 10% FBS for 1. Total cell lysates were prepared with ice-cold lysis buffer and the protein concentration was measured by Coomassie binding (Bio-Rad). Equal amounts of protein were added to each well of a G-LISA plate and incubated for 30 min at 4°C. The bound Rac was detected by adding an anti-Rac primary antibody and a secondary HRP-labeled antibody to each well. Finally, HRP detection reagents were added, and the resulting colorimetric reaction was quantified by measuring absorbance at 490 nm in a microplate spectrophotometer.

Atomic force microscopy (AFM)

Intracellular stiffness was measured by plating cells for 1 h on 18-mm soft- or stiff FN-coated polyacrylamide hydrogels with 10% FBS. The intracellular stiffness of single adherent cells was measured using a DAFM-2X Bioscope (Veeco) mounted on an Axiovert 100 microscope (Zeiss) in contact mode. Cells were indented against a standard silicon nitride cantilever (spring constant = 0.06 N/m) with a conical tip (40 nm in diameter). The elastic modulus (stiffness) was calculated by fitting the first 600 nm of tip deflection from the horizontal with the Hertz model for

a cone. The tip was placed near the edge of the cell to measure intracellular stiffness. Measurements were taken for 7–10 cells per condition, and the data were analyzed using a custom MATLAB script generously provided by Paul Janmey (University of Pennsylvania).

Fluorescence microscopy and quantification of f-actin intensity

Hydrogels were washed with PBS, and the cells were fixed in 3.7% formaldehyde (room temperature for 15 min) washed 3 times with PBS, and permeabilized with 0.4% Triton X-100 in PBS for 10 min, washed once with PBS, and blocked in 2% BSA and 0.2% Triton X-100 (30 min at room temperature). Primary antibodies to ATF3 (sc-188, Santa Cruz) and cyclin D1 (sc-450, Santa Cruz) were diluted at 100-fold in 2% BSA, 0.2% Triton X-100 and incubated with the cells for 1 h. The cells were then washed 3 times in PBS, 2%, BSA/0.2% Triton X-100, incubated with secondary antibody (diluted 100-fold) for 1 h at room temperature. The immunostained cells were then washed twice, and the coverslips were mounted using DAPI fluoromount G (0100-20, SouthernBiotech). To quantify F-actin signal intensity**,** fixed cells that had been stained for 1 h with Alexa Fluor™ 594 Phalloidin (A12381, ThermoFisher) in 2% BSA and 0.2% Triton X-100 were washed 3 times in PBS/0.2% Triton X-100 and mounted as described above.

Quantification of cell area was performed using ImageJ: a threshold was set to cover the whole cell surface, holes were filled using Process>Binary>Fill Holes commands, and then the individual cell areas were measured (Dang *et al.*, 2013). The phalloidin signal for each cell was measured, set on an arbitrary threshold based on the DMSO control cell intensity. F-actin intensity was then normalized to cell area for each cell.

RNASeq and bioinformatic analysis

Quadruplicate samples were generated for MEFs cultured in 4 different conditions: i) soft hydrogels, ii) stiff hydrogels, iii) stiff hydrogels with EHT1864, and iv) stiff hydrogels with CT04 as described above for "Acute Inhibition of Rac or Rho." Total RNA was extracted using Trizol reagent (Invitrogen), further purified with an RNeasy kit (74106, Qiagen), and prepared for RNA sequencing using TruSeq RNA Stranded mRNA (Illumina) and PE100. Sequencing coverage was ~$40x10^6$ reads. Salmon (https://combine-lab.github.io/salmon/) was used to count the data against the transcriptome defined in Gencode vM28, which was built on the genome GRCm39. Several Bioconductor packages (https://bioconductor.org) were used for subsequent steps. The transcriptome count data was annotated and summarized to the gene level with tximeta and further annotated with biomaRt. A Principal Component Analysis was performed with PCAtools, and this led to the exclusion of 1 of the 4 replicates of MEFs cultured on a soft hydrogel. Raw feature counts of the remaining 15 samples were normalized and analyzed for differential expression using DESeq2. Venn diagrams were generated from the DESeq2 output based on cut-offs of 0.32 $\log_2$ (approximately >1.25 $\log_{10}$) fold-change (positive or negative), <0.05 adjusted p-value, and >500 for base mean intensity. The genes regulated by ECM and Rac were compared to GO gene lists for transcription factors, transcription co-regulators and histone modifiers (GO terms 0003700, 0003712, and 0016570, respectively).

CRISPR/Cas9-mediated deletion of ATF3

The CRISPR sgRNA to mouse ATF3 (CCAGCGCAGAGGACAUCCGA) and ROSA26 (GAACAUAAAUGGCAACAUCU) were obtained from Synthego Corporation. The sgRNAs were diluted to 30 μM and Cas9 Nuclease to 20 μM. MEFs were seeded in 12-well plates and

grown to 70-80% confluency. Cells were transfected with RNPs (ribonucleoprotein) complexes using a NEON electroporation system (Invitrogen) and an RNP Complexes ratio of 9:1. Cells were electroporated with the following parameters: 1 pulse at 1350 V and 30 ms, then incubated in DMEM-10% FBS for 2-3 days. For clonal expansion, each well was trypsinized and diluted such that an average of 0.5 cells were plated per well in 96-well plates. Cells were cultured until they reach ~70% confluency and then subjected to Sanger sequencing. ROSA26 primers were ACATTTGGTCCTGCTTGAACA (forward) and ACATTTGGTCCTGCTTGAACA (reverse). ATF3 primers (for gRNA-1) were GTAGGCTGTCAGACCCCATG (forward) and GGTGCACACTATACCTGCTC (reverse). Sanger sequencing data were uploaded to the ICE CRISPR Analysis Tool (Synthego) to assess the ATF3 editing efficiency for each clone. Clones with a predicted knockout efficiency >95% were analyzed further by Western Blotting.

Statistical analysis

Statistical significance was determined using Prism (Graph-Pad) software. Graphs show means + SD unless the independent experiments generated means, in which case the error bars show SEM. T-tests were used to compare data unless noted otherwise in a figure legend. T-tests were 2-tailed unless testing for an effect in a specific direction. Unless specified in the figure legend, statistical significance was determined by t-tests with *$p<0.05$, **$p<0.01$, ***$p<0.001$, and ****$p<0.0001$. The reciprocal relationship between ATF3 and cyclin D1 was assessed using the correlation coefficient, R^2.

ACKNOWLEDGEMENTS

We John Tobias (University of Pennsylvania) for assistance with the bioinformatic analysis This work was supported by NIH grant HL137232 to RKA, by the Center for Engineering MechanoBiology, a National Science Foundation Science and Technology Center under grant agreement CMMI 15-48571, and by EMBO post-doctoral EMBO ALTF 1082-2016 to ID. YB was supported by American Heart Association Career Development Award 18CDA34080415.

BIBLIOGRAPHY

Allan, AL, Albanese, C, Pestell, RG, and LaMarre, J (2001). Activating transcription factor 3 induces DNA synthesis and expression of cyclin D1 in hepatocytes. J Biol Chem 276, 27272–27280.

Aragona, M, Panciera, T, Manfrin, A, Giulitti, S, Michielin, F, Elvassore, N, Dupont, S, and Piccolo, S (2013). A mechanical checkpoint controls multicellular growth through YAP/TAZ regulation by actin-processing factors. Cell 154, 1047–1059.

Assoian, RK, and Klein, EA (2008). Growth control by intracellular tension and extracellular stiffness. Trends Cell Biol 7, 24–27.

Assoian, RK, and Schwartz, MA (2001). Coordinate signaling by integrins and receptor tyrosine kinases in the regulation of G1 phase cell-cycle progression. Curr Opin Genet Dev 11, 48–53.

Bae, YH, Mui, KL, Hsu, BY, Liu, S-L, Cretu, A, Razinia, Z, Xu, T, Puré, E, and Assoian, RK (2014). A FAK-Cas-Rac-lamellipodin signaling module transduces extracellular matrix stiffness into mechanosensitive cell cycling. Sci Signal 7, ra57.

Boudreau, NJ, and Jones, PL (1999). Extracellular matrix and integrin signalling: the shape of things to come. Biochem J 339, 481.

Bourgot, I, Primac, I, Louis, T, Noël, A, and Maquoi, E (2020). Reciprocal Interplay Between Fibrillar Collagens and Collagen-Binding Integrins: Implications in Cancer Progression and Metastasis. Front Oncol 10, 1488.

Brazzo, JA, Biber, JC, Nimmer, E, Heo, Y, Ying, L, Zhao, R, Lee, K, Krause, M, and Bae, Y (2021). Mechanosensitive expression of lamellipodin promotes intracellular stiffness, cyclin expression and cell proliferation. J Cell Sci 134, jcs257709.

Burridge, K, and Guilluy, C (2016). Focal adhesions, stress fibers and mechanical tension. Exp Cell Res 343, 14–20.

Burridge, K, and Wennerberg, K (2004). Rho and Rac Take Center Stage. Cell 116, 167–179.

Burridge, K, and Wittchen, ES (2013). The tension mounts: Stress fibers as force-generating mechanotransducers. J Cell Biol 200, 9–19.

Cerione, RA (2004). Cdc42: new roads to travel. Trends Cell Biol 14, 127–132.

Cretu, A, Castagnino, P, and Assoian, R (2010). Studying the effects of matrix stiffness on cellular function using acrylamide-based hydrogels. J Vis Exp. 42, 2089.

Dahl, KN, Ribeiro, AJS, and Lammerding, J (2008). Nuclear shape, mechanics, and mechanotransduction. Circ Res 102, 1307–1318.

Dang, I et al. (2013). Inhibitory signalling to the Arp2/3 complex steers cell migration. Nature 503, 281–284.

Dinh, TA et al. (2022). A framework for fibrolamellar carcinoma research and clinical trials. Nat Rev Gastroenterol Hepatol 19, 328–342.

Discher, DE, Janmey, P, and Wang, YL (2005). Tissue cells feel and respond to the stiffness of their substrate. Science 310, 1139–1143.

Dupont, S et al. (2011). Role of YAP/TAZ in mechanotransduction. Nature 474, 179–183.

Duprez, DA, and Cohn, JN (2007). Arterial stiffness as a risk factor for coronary atherosclerosis. Curr Atheroscler Rep 9, 139–144.

Engler, AJ, Sen, S, Sweeney, HL, and Discher, DE (2006). Matrix elasticity directs stem cell lineage specification. Cell 126, 677–689.

Fan, F et al. (2002). ATF3 induction following DNA damage is regulated by distinct signaling pathways and over-expression of ATF3 protein suppresses cells growth. Oncogene 21, 7488–7496.

Gehler, S, Ponik, SM, Riching, KM, and Keely, PJ (2013). Bi-directional signaling: extracellular matrix and integrin regulation of breast tumor progression. Crit Rev Eukaryot Gene Expr 23, 139–157.

Geiger, B, and Bershadsky, A (2001). Assembly and mechanosensory function of focal contacts. Curr Opin Cell Biol 13, 584–592.

Geiger, B, and Yamada, KM (2011). Molecular Architecture and Function of Matrix Adhesions. Cold Spring Harb Perspect Biol 3, a005033–a005033.

Hai, T, and Hartman, MG (2001). The molecular biology and nomenclature of the activating transcription factor/cAMP responsive element binding family of transcription factors: activating transcription factor proteins and homeostasis. Gene 273, 1–11.

Hai, T, Liu, F, Coukos, WJ, and Green, MR (1989). Transcription factor ATF cDNA clones: an extensive family of leucine zipper proteins able to selectively form DNA-binding heterodimers. Genes Dev 3, 2083–2090.

Hall, A (2005). Rho GTPases and the control of cell behaviour. Biochem Soc Trans 33, 891–895.

Horton, ER, Humphries, JD, James, J, Jones, MC, Askari, JA, and Humphries, MJ (2016). The integrin adhesome network at a glance. J Cell Sci 129, 4159.

James, CG, Woods, A, Underhill, TM, and Beier, F (2006). The transcription factor ATF3 is upregulated during chondrocyte differentiation and represses cyclin D1 and A gene transcription.

BMC Mol Biol 7, 30.

Jang, JW et al. (2017). RAC-LATS1/2 signaling regulates YAP activity by switching between the YAP-binding partners TEAD4 and RUNX3. Oncogene 36, 999–1011.

Janmey, PA, Wells, RG, Assoian, RK, Mcculloch, CA, Group, D, and Building, F (2015). From tissue mechanics to transcription factors. Differentiation 86, 112–120.

Keely, PJ (2011). Mechanisms by which the extracellular matrix and integrin signaling act to regulate the switch between tumor suppression and tumor promotion. J Mammary Gland Biol Neoplasia 16, 205–219.

Kirby, TJ, and Lammerding, J (2018). Emerging views of the nucleus as a cellular mechanosensor. Nat Cell Biol 20, 373–381.

Klein, EA, Yin, L, Kothapalli, D, Castagnino, P, Byfield, FJ, Xu, T, Levental, I, Hawthorne, E, Janmey, PA, and Assoian, RK (2009). Cell-cycle control by physiological matrix elasticity and in vivo tissue stiffening. Curr Biol 19, 1511–1518.

Klein, EA, Yung, Y, Castagnino, P, Kothapalli, D, and Assoian, RK (2007). Cell adhesion, cellular tension, and cell cycle control. Methods Enzym 426, 155–175.

Kothapalli, D et al. (2012). Cardiovascular Protection by ApoE and ApoE-HDL Linked to Suppression of ECM Gene Expression and Arterial Stiffening. Cell Rep 2, 1259–1271.

Ku, HC, and Cheng, CF (2020). Master Regulator Activating Transcription Factor 3 (ATF3) in Metabolic Homeostasis and Cancer. Front Endocrinol (Lausanne) 11, 556.

Larsen, M, Artym, V V., Green, JA, and Yamada, KM (2006). The matrix reorganized: extracellular matrix remodeling and integrin signaling. Curr Opin Cell Biol 18, 463–471.

Lawson, CD, and Burridge, K (2014). The on-off relationship of Rho and Rac during integrin-mediated adhesion and cell migration. Small GTPases 5, e27958.

Lee, JW, and Juliano, R (2004). Mitogenic signal transduction by integrin- and growth factor receptor-mediated pathways. Mol Cells 17, 188–202.

Lessey, EC, Guilluy, C, and Burridge, K (2012). From mechanical force to RhoA activation. Biochemistry 51, 7420–7432.

Levental, KR et al. (2009). Matrix crosslinking forces tumor progression by enhancing integrin signaling. Cell 139, 891–906.

Liu, F, Mih, JD, Shea, BS, Kho, AT, Sharif, AS, Tager, AM, and Tschumperlin, DJ (2010). Feedback amplification of fibrosis through matrix stiffening and COX-2 suppression. J Cell Biol 190, 693–706.

Lu, D, Wolfgang, CD, and Hai, T (2006). Activating transcription factor 3, a stress-inducible gene, suppresses Ras-stimulated tumorigenesis. J Biol Chem 281, 10473–10481.

Maneshi, P, Mason, J, Dongre, M, and Öhlund, D (2021). Targeting Tumor-Stromal Interactions in Pancreatic Cancer: Impact of Collagens and Mechanical Traits. Front Cell Dev Biol 9, 787485.

Miralles, F, Posern, G, Zaromytidou, A-I, and Treisman, R (2003). Actin dynamics control SRF activity by regulation of its coactivator MAL. Cell 113, 329–342.

Parmacek, MS (2007). Myocardin-related transcription factors: critical coactivators regulating cardiovascular development and adaptation. Circ Res 100, 633–644.

Pasapera, AM, Plotnikov, S V, Fischer, RS, Case, LB, Egelhoff, TT, and Waterman, CM (2014). Rac1-Dependent Phosphorylation and Focal Adhesion Recruitment of Myosin IIA Regulates Migration and Mechanosensing. Curr Biol 25, 175–186.

Paszek, MJ et al. (2005). Tensional homeostasis and the malignant phenotype. Cancer Cell 8, 241–254.

Perez, S, Vial, E, Van Dam, H, and Castellazzi, M (2001). Transcription factor ATF3 partially transforms chick embryo fibroblasts by promoting growth factor-independent proliferation. Oncogene 20, 1135–1141.

Piersma, B, Hayward, MK, and Weaver, VM (2020). Fibrosis and cancer: A strained relationship. Biochim Biophys Acta Rev Cancer 1873, 188356.

Pipes, GCT, Creemers, EE, and Olson, EN (2006). The myocardin family of transcriptional coactivators: Versatile regulators of cell growth, migration, and myogenesis. Genes Dev 20, 1545–1556.

Provenzano, PP, and Keely, PJ (2011). Mechanical signaling through the cytoskeleton regulates cell proliferation by coordinated focal adhesion and Rho GTPase signaling. J Cell Sci 124, 1195–1205.

Raftopoulou, M, and Hall, A (2004). Cell migration: Rho GTPases lead the way. Dev Biol 265, 23–32.

Razinia, Z, Castagnino, P, Xu, T, Vázquez-Salgado, A, Puré, E, and Assoian, RK (2017). Stiffness-dependent motility and proliferation uncoupled by deletion of CD44. Sci Rep 7, 16499.

Reid, SE et al. (2017). Tumor matrix stiffness promotes metastatic cancer cell interaction with the endothelium. EMBO J 36, 2373–2389.

Resnitzky, D, and Reed, SI (1995). Different roles for cyclins D1 and E in regulation of the G1-

to-S transition. Mol Cell Biol 15, 3463–3469.

Ridley, AJ (2006). Rho GTPases and actin dynamics in membrane protrusions and vesicle trafficking. Trends Cell Biol 16, 522–529.

Ridley, AJ (2015). Rho GTPase signalling in cell migration. Curr Opin Cell Biol 36, 103–112.

Rohini, M, Haritha Menon, A, and Selvamurugan, N (2018). Role of activating transcription factor 3 and its interacting proteins under physiological and pathological conditions. Int J Biol Macromol 120, 310–317.

Sahai, E, and Marshall, CJ (2003). Differing modes of tumour cell invasion have distinct requirements for Rho/ROCK signalling and extracellular proteolysis. Nat Cell Biol 5, 711–719.

Sastry, SK, and Burridge, K (2000). Focal adhesions: a nexus for intracellular signaling and cytoskeletal dynamics. Exp Cell Res 261, 25–36.

Sherr, CJ (1993). Mammalian G1 cyclins. Cell 73, 1059–1065.

Sherr, CJ (1995). D-type cyclins. Trends Biochem Sci 20, 187–190.

Shutova, MS, Asokan, SB, Talwar, S, Assoian, RK, Bear, JE, and Svitkina, TM (2017). Self-sorting of nonmuscle myosins IIA and IIB polarizes the cytoskeleton and modulates cell motility. J Cell Biol 216, 2877-2889.

Sotiropoulos, A, Gineitis, D, Copeland, J, and Treisman, R (1999). Signal-regulated activation of serum response factor is mediated by changes in actin dynamics. Cell 98, 159-69.

Sun, B (2021). The mechanics of fibrillar collagen extracellular matrix. Cell Reports Phys Sci 2, 100515.

Suresh, S (2007). Biomechanics and biophysics of cancer cells. Acta Biomater 3, 413–438.

Swift, J, and Discher, DE (2014). The nuclear lamina is mechano-responsive to ECM elasticity in mature tissue. J Cell Sci 127, 3005–3015.

Talwar, S, Kant, A, Xu, T, Shenoy, VB, and Assoian, RK (2021). Mechanosensitive smooth muscle cell phenotypic plasticity emerging from a null state and the balance between Rac and Rho. Cell Rep 35, 109019.

Tang, VW (2020). Collagen, stiffness, and adhesion: the evolutionary basis of vertebrate mechanobiology. Mol Biol Cell 31, 1823–1834.

Tung, JC, Barnes, JM, Desai, SR, Sistrunk, C, Conklin, MW, Schedin, P, Eliceiri, KW, Keely, PJ, Seewaldt, VL, and Weaver, VM (2015). Tumor mechanics and metabolic dysfunction. Free Radic Biol Med 79, 269–280.

Wang, N, Tytell, JD, and Ingber, DE (2009). Mechanotransduction at a distance: mechanically coupling the extracellular matrix with the nucleus. Nat Rev Mol Cell Biol 2009 101 10, 75–82.

Wei, SC et al. (2015). Matrix stiffness drives epithelial-mesenchymal transition and tumour metastasis through a TWIST1-G3BP2 mechanotransduction pathway. Nat Cell Biol 17, 678–688.

Wei, SC, and Yang, J (2016). Forcing through Tumor Metastasis: The Interplay between Tissue Rigidity and Epithelial-Mesenchymal Transition. Trends Cell Biol 26, 111–120.

Weinberg, RA (1995). The retinoblastoma protein and cell cycle control. Cell 81, 323–330.

Wolfenson, H, Yang, B, and Sheetz, MP (2019). Steps in Mechanotransduction Pathways that Control Cell Morphology. Annu Rev Physiol 81, 585-605.

Yeung, T, Georges, PC, Flanagan, LA, Marg, B, Ortiz, M, Funaki, M, Zahir, N, Ming, W, Weaver, V, and Janmey, PA (2005). Effects of substrate stiffness on cell morphology, cytoskeletal structure, and adhesion. Cell Motil Cytoskelet 60, 24–34.

Zaidel-Bar, R, Itzkovitz, S, Ma'ayan, A, Iyengar, R, and Geiger, B (2007). Functional atlas of the integrin adhesome. Nat Cell Biol 9, 858.

Zajac, AL, and Discher, DE (2008). Cell differentiation through tissue elasticity-coupled, myosin-driven remodeling. Curr Opin Cell Biol 20, 609–615.

Zhang, W, Zhang, S, Zhang, W, Yue, Y, Qian, W, and Wang, Z (2021). Matrix stiffness and its influence on pancreatic diseases. Biochim Biophys Acta Rev Cancer 1876, 188583.

Zhao, XH, Laschinger, C, Arora, P, Szaszi, K, Kapus, A, and McCulloch, CA (2007). Force activates smooth muscle alpha-actin promoter activity through the Rho signaling pathway. J Cell Sci 120, 1801–1809.

Zohn, IM, Campbell, SL, Khosravi-Far, R, Rossman, KL, and Der, CJ (1998). Rho family proteins and Ras transformation: the RHOad less traveled gets congested. Oncogene 17, 1415–1438.

FIGURE LEGENDS

Figure 1. **Rac and Rho inhibition similarly reduce f-actin staining cell stiffness.** Serum-starved MEFs pre-incubated with CT04 (Rho inhibitor) or EHT1864 (Rac inhibitor) were plated on FN-coated hydrogels and stimulated with 10% FBS for 1 h. **(A)** Rho-family GTPase activity was measured by G-LISA and plotted relative to the activity on the soft hydrogels (n=4). Graphs show mean + SEM. **(B)** Maximum projection images of phalloidin-stained MEFs taken by confocal microscopy. Scale bar = 50 µm. **(C)** Quantification of phalloidin-stained MEFs was measured and normalized to cell area with Image J. Results show mean and SD; n=137 (DMSO), 165 (EHT1864), and 152 (CT04) cells accrued from 3 independent experiments. **(D)** Cell areas were measured with ImageJ. Results show mean and SD; n=259 (DMSO), 308 (EHT1864), and 222 (CT04) cells accrued from 3 independent experiments. **(E)** Cell stiffness was determined by AFM. The graph shows mean + SEM (n=34 cells per condition accrued over 4 independent experiments).

Figure 2. Rac drives the initial genome-wide response to ECM stiffness and preferentially represses ATF3. (A-B) Venn diagrams of differentially expressed genes in MEFs cultured with 10% FBS for 1 hour on stiff versus soft hydrogels, stiff hydrogels ± EHT1864, or stiff hydrogels ± CT04. **(C-D)** The genes regulated by ECM and Rac (163 stiffness-stimulated/EHT-inhibited and 123 stiffness-inhibited/EHT-stimulated genes; see Figs. 2A and B, respectively) were compared to GO gene lists for transcription factors, transcription co-regulators and histone modifiers. **(E-F)** Log2 fold-changes and adjusted p-values of the genes regulated by ECM stiffness/Rac and contained within the GO terms described above. **(G)** Serum-starved MEFs were plated on soft or stiff FN-coated hydrogels with 10% FBS for 1 h in the presence of DMSO (Ctrl), EHT1864, or CT04. Total RNA was extracted, and ATF3 mRNA levels were quantified by RT-qPCR. The graph show mean + SEM (n=4). **(H-I)** Serum-starved MEFs were cultured as in panel C but with DMSO or EHT1864. Cell lysates were analyzed by western blot; results from 6 independent experiments were quantified using Image J. The graph shows mean + SD.

Figure 3. Dose-dependent effects of ECM stiffness on ATF3 and cyclin D1 mRNAs. (A) Serum-starved MEFs were seeded on FN-coated hydrogels of increasing stiffness (approximately 2, 8, 15, and 25 kPa) and incubated in DMEM-10% FBS for 1 h prior to cell lysis and analysis of Rac-GTP levels by G-LISA. Results show mean ± SEM (n=4). **(B-C)** Cells were treated as in panel A but incubated for 9 h prior to determination of ATF3 and cyclin D1 mRNA levels by RT-qPCR (n=3). Statistical significance for each panel was determined by ANOVA; asterisks show the results of Dunnett's post-tests performed relative to the softest ECM (2-4 kPa) ECM.

Figure 4. ATF3 repression linked to stiffness-dependent cyclin D1 expression. (A) Serum-starved MEFs were plated on soft or stiff FN-coated hydrogels in DMEM-10% FBS and treated with either vehicle (DMSO) or EHT1864 for 9 h. Cells were lysed, and the levels of both ATF3 mRNA and cyclin D1 mRNA were determined by RT-qPCR from the same lysates. Results show mean + SEM (n=3). R^2 is the correlation coefficient. **(B)** MEFs were infected with adenoviruses encoding GFP (control) or Rac^{V12} and serum-starved. The cells were then cultured and analyzed by RT-qPCR as in panels A. Results show mean + SEM (n=3). **(C)** MEFs were infected with adenoviruses (Ad) encoding GFP (control) or ATF3. Cells were serum-starved and plated on FN-coated hydrogels for 15 h. The cells were analyzed by western blot for the level of cyclin D1 and ATF3 with GAPDH as the loading control. **(D)** Quantification of western blot results in C; the

graph shows mean + SD (n=3). (**E)** Representative images of ROSA (control) and ATF3 KO MEFs that had been serum-starved and plated on stiff FN-coated hydrogels in DMEM-10% FBS for 9 h before fixation and immunostaining for cyclin D1. **(F)** Cyclin D1 staining intensity was quantified with Image J from ~ 300 cells per condition accrued from 2 independent experiments. The dot plot shows results for each cell and the mean. (**G)** S-phase entry was analyzed by EdU incorporation in 4 different ROSA (control) clones and 4 different ATF3 KO clones after serum-starvation incubation on stiff FN-coated hydrogels in DMEM-10% FBS for 24 h. Results show mean + SD; n=7 for the ROSA clones and 8 for the ATF3 KO clones. **(H)** Model showing how cyclin D1 is regulated by ECM stiffness and Rac through ATF3.

Figure 1

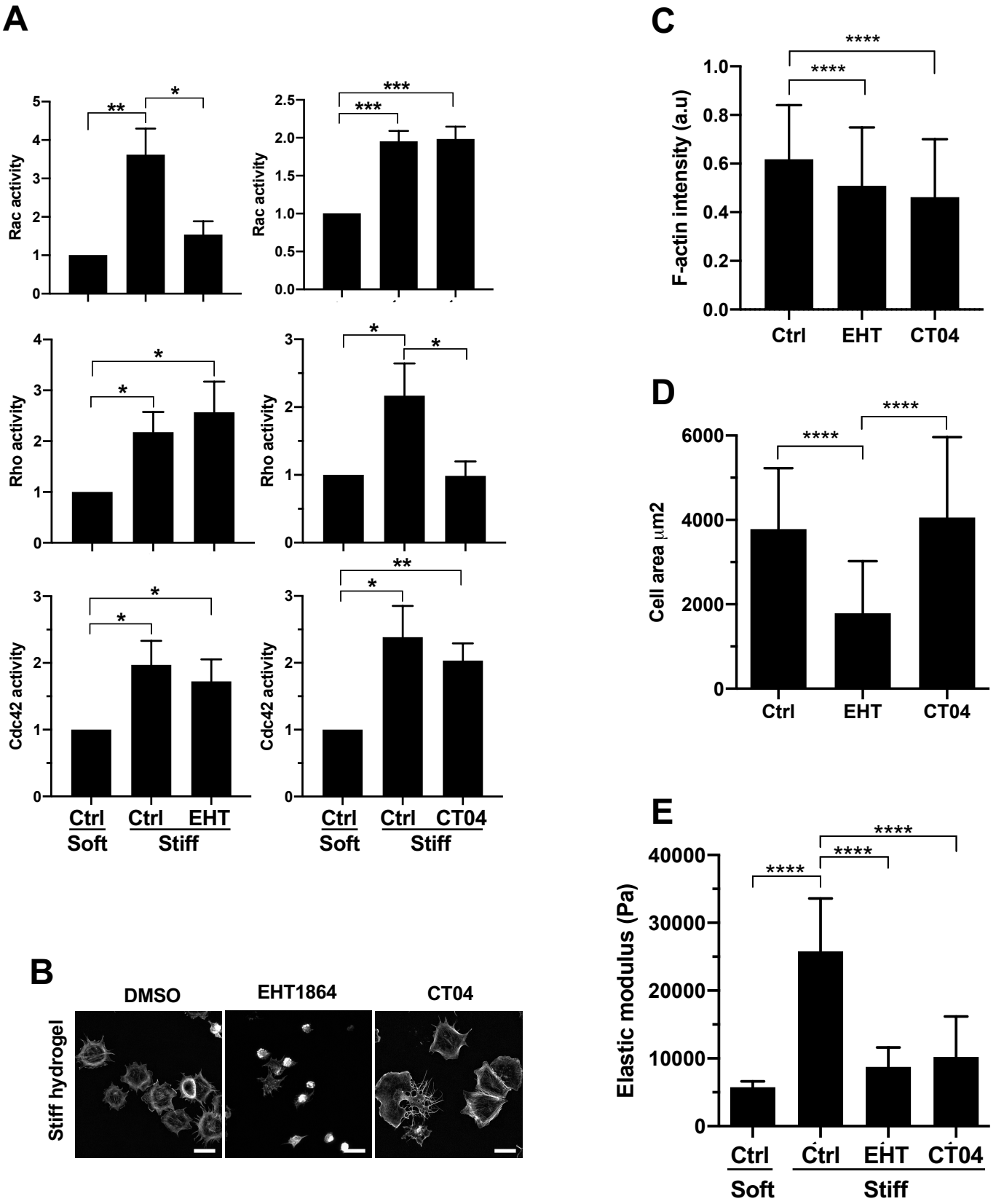
A
Rac activity
Rho activity
Cdc42 activity
Ctrl
Ctrl
EHT
Soft
Stiff
Ctrl
Ctrl
CT04
Soft
Stiff
B
DMSO
EHT1864
CT04
Stiff hydrogel
C
F-actin intensity (a.u)
Ctrl
EHT
CT04
D
Cell area µm2
Ctrl
EHT
CT04
E
Elastic modulus (Pa)
Ctrl
Ctrl
EHT
CT04
Soft
Stiff

Figure 2

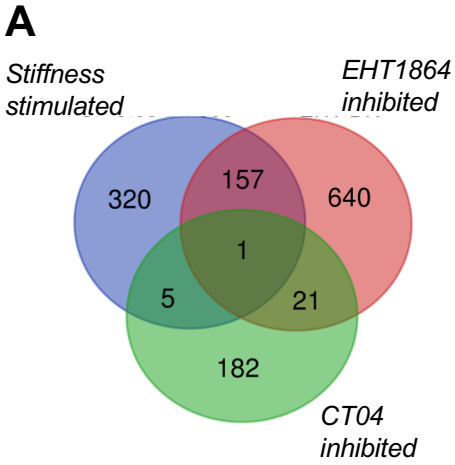
A
Stiffness stimulated
EHT1864 inhibited
CT04 inhibited
320
157
640
1
5
21
182

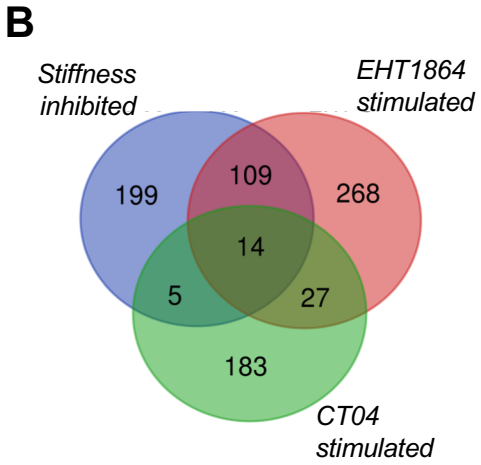
B
Stiffness inhibited
EHT1864 stimulated
CT04 stimulated
199
109
268
14
5
27
183

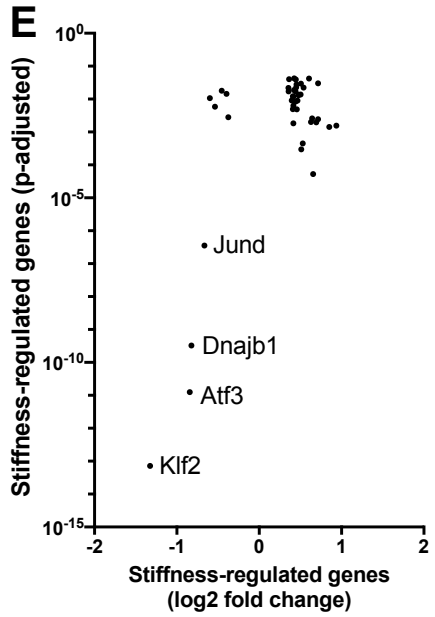
E
Stiffness-regulated genes (p-adjusted)
Stiffness-regulated genes (log2 fold change)
Jund
Dnajb1
Atf3
Klf2

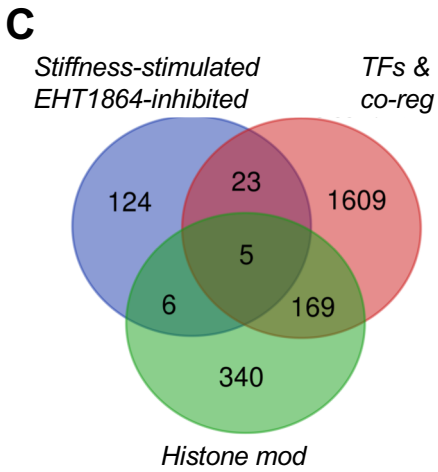
C
Stiffness-stimulated EHT1864-inhibited
TFs & co-reg
Histone mod
124
23
1609
5
6
169
340

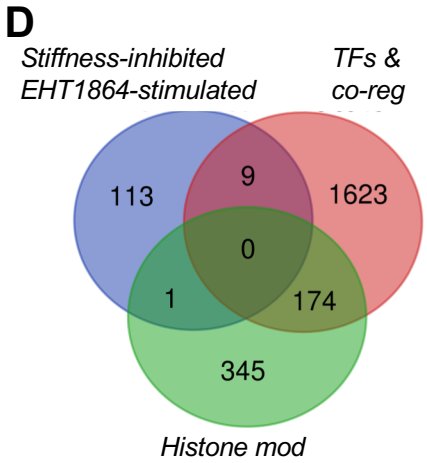
D
Stiffness-inhibited EHT1864-stimulated
TFs & co-reg
Histone mod
113
9
1623
0
1
174
345

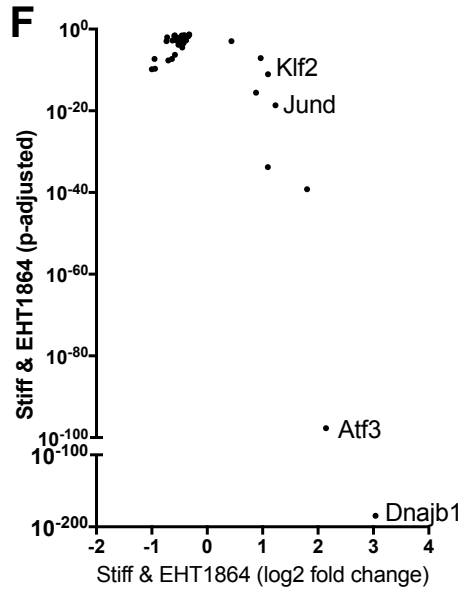
F
Stiff & EHT1864 (p-adjusted)
Stiff & EHT1864 (log2 fold change)
Klf2
Jund
Atf3
Dnajb1

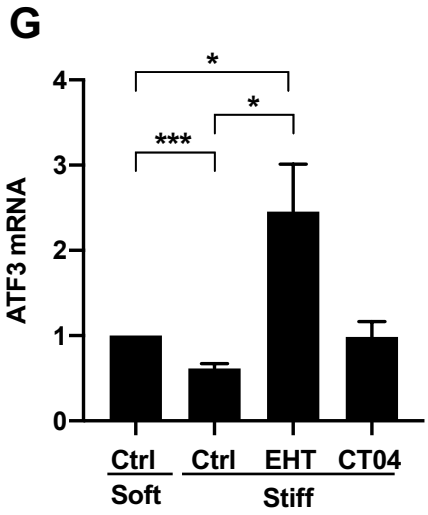
G
ATF3 mRNA
Ctrl
Ctrl
EHT
CT04
Soft
Stiff

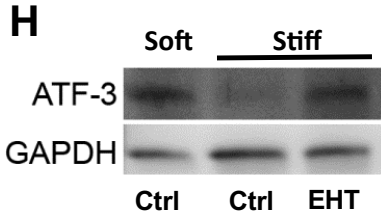
H
Soft
Stiff
ATF-3
GAPDH
Ctrl
Ctrl
EHT

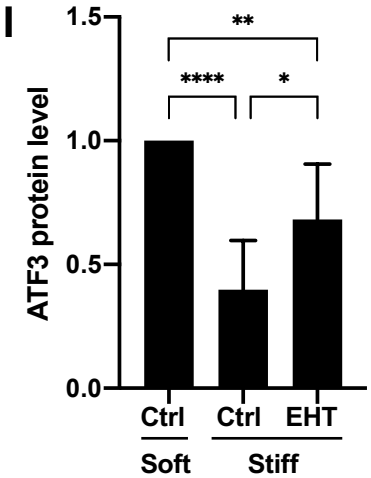
I
ATF3 protein level
Ctrl
Ctrl
EHT
Soft
Stiff

Figure 3

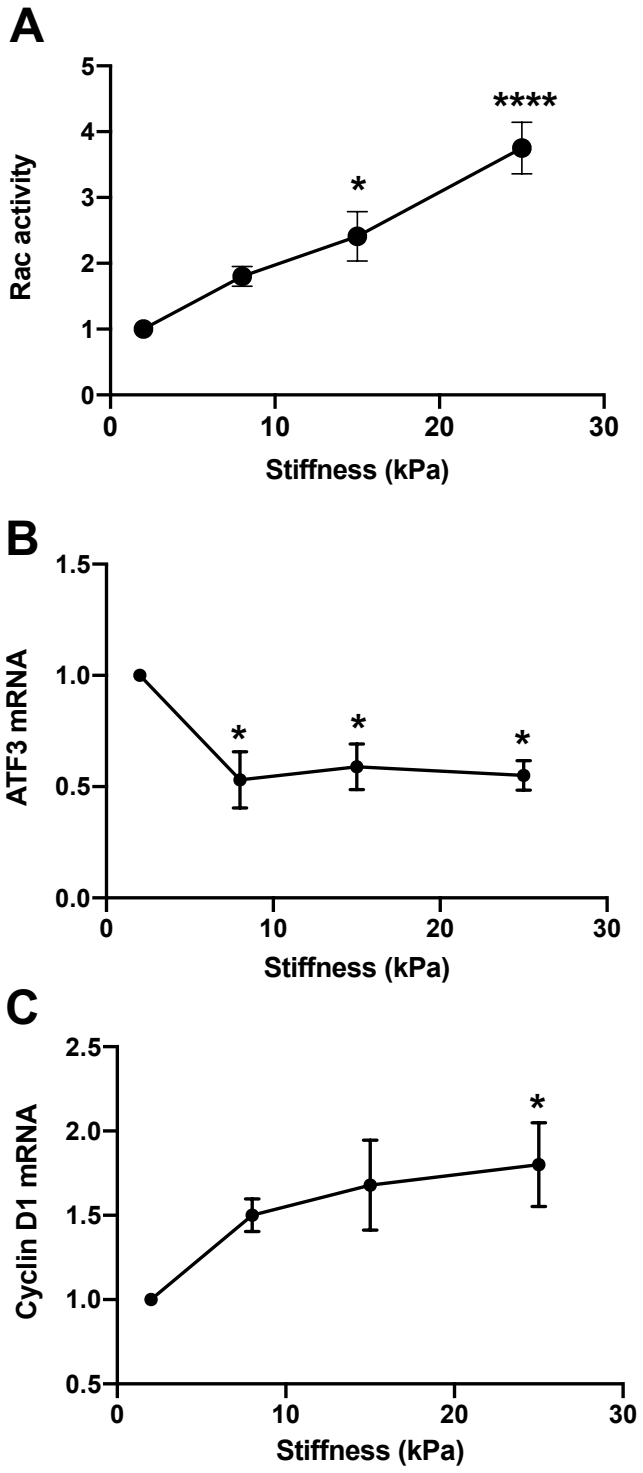
A
Rac activity
5
4
3
2
1
0
****
*
0
10
20
30
Stiffness (kPa)
B
ATF3 mRNA
1.5
1.0
0.5
0.0
*
*
*
0
10
20
30
Stiffness (kPa)
C
Cyclin D1 mRNA
2.5
2.0
1.5
1.0
0.5
*
0
10
20
30
Stiffness (kPa)

Figure 4

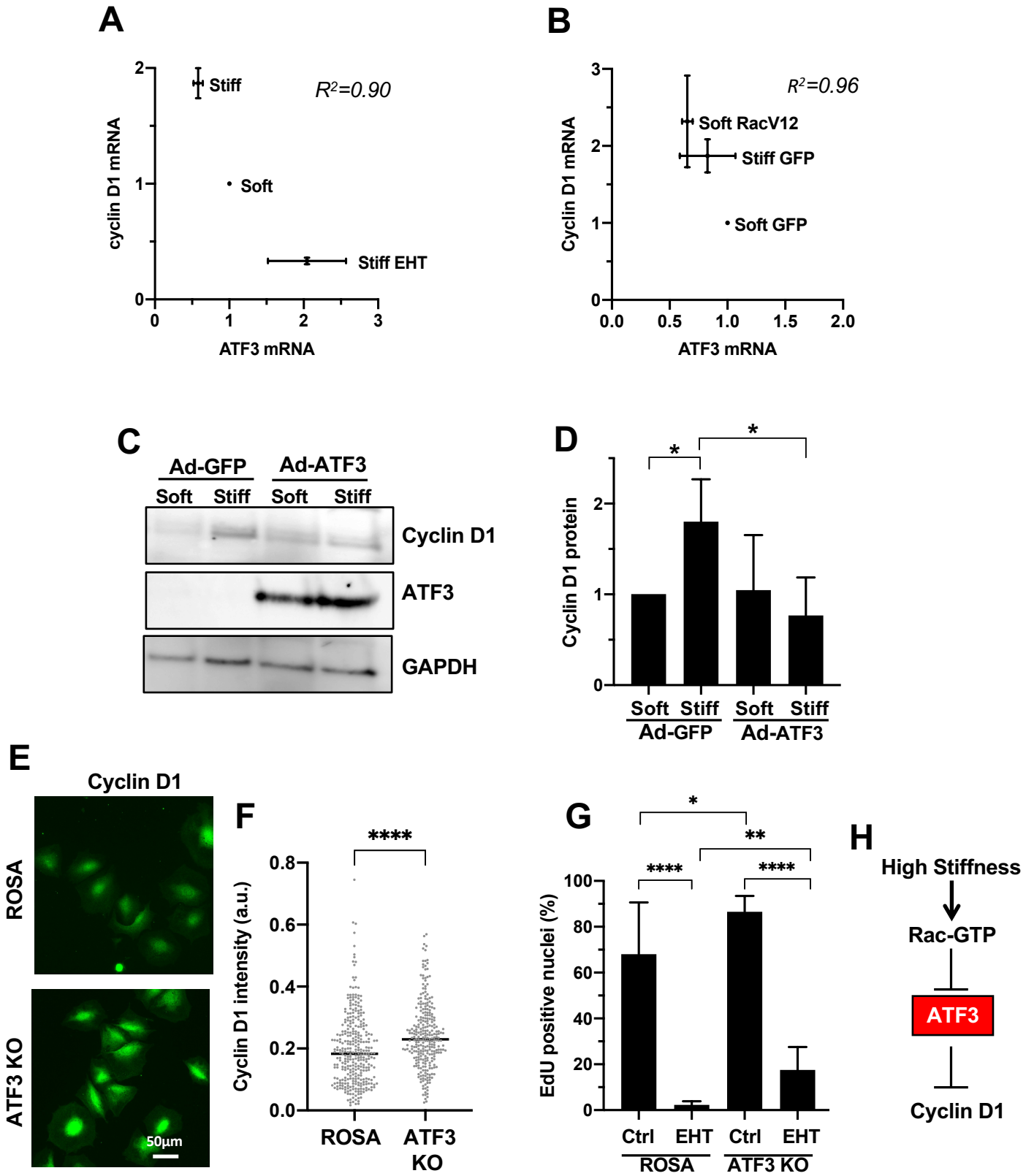
A
Stiff
Soft
Stiff EHT
R²=0.90
cyclin D1 mRNA
ATF3 mRNA
B
Soft RacV12
Stiff GFP
Soft GFP
R²=0.96
Cyclin D1 mRNA
ATF3 mRNA
C
Ad-GFP
Ad-ATF3
Soft
Stiff
Soft
Stiff
Cyclin D1
ATF3
GAPDH
D
Cyclin D1 protein
Soft
Stiff
Soft
Stiff
Ad-GFP
Ad-ATF3
E
Cyclin D1
ROSA
ATF3 KO
50µm
F
Cyclin D1 intensity (a.u.)
ROSA
ATF3 KO
G
EdU positive nuclei (%)
Ctrl
EHT
Ctrl
EHT
ROSA
ATF3 KO
H
High Stiffness
Rac-GTP
ATF3
Cyclin D1